AGU PUBLICATIONS

Geochemistry, Geophysics, Geosystems

RESEARCH ARTICLE
10.1002/2014GC005359

Special Section:
Subduction processes in Central America with an emphasis on CRISP results

Interplate seismicity at the CRISP drilling site: The 2002 Mw 6.4 Osa Earthquake at the southeastern end of the Middle America Trench

Ivonne G. Arroyo[1], Ingo Grevemeyer[1], Cesar R. Ranero[2], and Roland von Huene[3]

[1]GEOMAR Helmholtz-Zentrum für Ozeanforschung Kiel, Kiel, Germany, [2]ICREA, Institute of Marine Sciences, CSIC, Barcelona, Spain, [3]Department of Geology, University of California, Davis, Davis, California, USA

Key Points:
- A large subduction earthquake located in the area of interplate drilling project
- Most of the seismic energy was radiated at shallow depth below the margin slope
- Cocos Ridge subduction creates conditions for shallower interplate seismogenesis

Correspondence to:
I. G. Arroyo,
iarroyo@geomar.de

Citation:
Arroyo, I. G., I. Grevemeyer, C. R. Ranero, and R. von Huene (2014), Interplate seismicity at the CRISP drilling site: The 2002 Mw 6.4 Osa Earthquake at the southeastern end of the Middle America Trench, *Geochem. Geophys. Geosyst.*, *15*, 3035–3050, doi:10.1002/2014GC005359.

Received 1 APR 2014
Accepted 4 JUL 2014
Accepted article online 10 JUL 2014
Published online 31 JUL 2014

Abstract We investigate potential relations between variations in seafloor relief and age of the incoming plate and interplate seismicity. Westward from Osa Peninsula in Costa Rica, a major change in the character of the incoming Cocos Plate is displayed by abrupt lateral variations in seafloor depth and thermal structure. Here a Mw 6.4 thrust earthquake was followed by three aftershock clusters in June 2002. Initial relocations indicate that the main shock occurred fairly trenchward of most large earthquakes along the Middle America Trench off central Costa Rica. The earthquake sequence occurred while a temporary network of OBH and land stations ~80 km to the northwest were deployed. By adding readings from permanent local stations, we obtain uncommon *P* wave coverage of a large subduction zone earthquake. We relocate this catalog using a nonlinear probabilistic approach within both, a 1-D and a 3-D *P* wave velocity models. The main shock occurred ~25 km from the trench and probably along the plate interface at 5–10 km depth. We analyze teleseismic data to further constrain the rupture process of the main shock. The best depth estimates indicate that most of the seismic energy was radiated at shallow depth below the continental slope, supporting the nucleation of the Osa earthquake at ~6 km depth. The location and depth coincide with the plate boundary imaged in prestack depth-migrated reflection lines shot near the nucleation area. Aftershocks propagated downdip to the area of a 1999 Mw 6.9 sequence and partially overlapped it. The results indicate that underthrusting of the young and buoyant Cocos Ridge has created conditions for interplate seismogenesis shallower and closer to the trench axis than elsewhere along the central Costa Rica margin.

1. Introduction

The role of the thermal state and abrupt changes in seafloor relief and/or in sediment-cover thickness of subducting plates is widely discussed as potentially influencing the seismogenic behavior of plate boundary faults [e.g., *Abercrombie et al.*, 2001; *Oleskevich et al.*, 1999; *Wang and Bilek*, 2014]. The subduction zone of Costa Rica displays marked along-trench changes in the character of the incoming oceanic Cocos Plate. Three plate segments underthrust the margin (Figure 1): a smooth segment underthrusts the Nicoya Peninsula, a segment spotted by large 20–30 km wide and 2–3 km tall conical seamounts and ridges underthrusts central Costa Rica, and the broad swell of the Cocos Ridge underthrusts the Osa Peninsula. Sediment thickness along the trench does not differ in a regular pattern, but the Cocos Ridge is formed by somewhat younger, thicker, and hotter crust [*Barckhausen et al.*, 2001; *Harris et al.*, 2010]. Conceptually, this could produce an abrupt lateral change of the physical state of the material along the plate boundary fault. The thicker crust also initiates subduction at a slightly shallower angle, which might also cause different stresses at the plate boundary in this segment leading to a variation in the degree of mechanical coupling, as suggested by limited GPS data [*LaFemina et al.*, 2009]. In addition, the Costa Rica megathrust is characterized by subduction erosion processes [*Ranero and von Huene*, 2000; *von Huene et al.*, 2004; *Vannucchi et al.*, 2013], which potentially imply that some of the hypotheses discussed for seismogenesis at plate boundary faults of accretionary systems do not operate here [*Ranero et al.*, 2008]. We have analyzed one of the best recorded earthquake data sets at the northwestern flank of the Cocos Ridge to investigate whether the change in incoming plate parameters leads to a change in seismic behavior of the plate boundary fault, when compared to the rest of Costa Rica.

On 16 June 2002, a Mw 6.4 earthquake rupture nucleated roughly 30 km west of the Osa Peninsula (Figure 1). The Global Centroid Moment Tensor solution (gCMT) [*Dziewonski et al.*, 1981] indicates an underthrusting

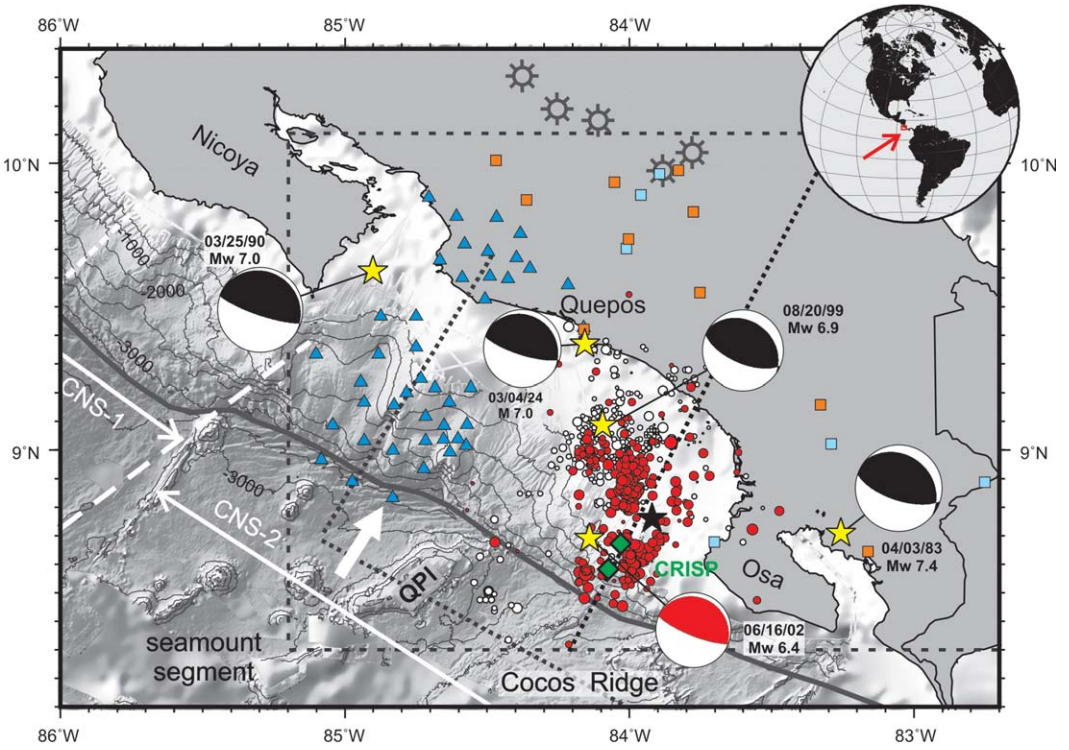

Figure 1. Tectonic setting and seismological networks that recorded the 2002 Mw 6.4 Osa earthquake sequence in the Costa Rican Central Pacific margin. The blue triangles represent the SFB574 temporal network, consisting on land and ocean-bottom stations that operated from April to October 2002. Additional readings from some stations of the permanent networks RSN (orange squares) and OVSICORI (blue squares) improve the coverage. Preliminary locations of the Osa sequence are shown in red. The white circles are aftershocks of the 1999 Mw 6.9 Quepos sequence after *DeShon et al*. [2003]. Bathymetry (exaggerated), including contours every 500 m, and main tectonic segments after *von Huene et al*. [2000] and *Barckhausen et al*. [2001], respectively. The Cocos Plate oceanic crust subducting in this margin segment was formed at the Cocos-Nazca Spreading Center (CNS). The Cocos Plate motion azimuth (thick white arrow) is from *DeMets et al*. [1994]. Radiating circles denote Holocene volcanoes. The dashed box marks the boundaries of the 3-D velocity model constructed from wide-angle profiles (dotted lines) [*Ye et al*., 1996; *Stavenhagen et al*., 1998; *Walther*, 2003] and other information, used to relocate seismicity with NonLinLoc. Yellow stars represent the epicenters of recent large earthquakes associated to subduction of bathymetric highs: 1924 M 7.0 Quepos [*Fernández Arce and Doser*, 2009], 1983 Mw 7.4 Golfito [*Adamek et al*., 1987], 1990 Mw 7.0 Cobano [*Husen et al*., 2002], 1999 Mw 6.9 Quepos (location from RSN), and 2002 Mw 6.4 Osa (gCMT location). Global Centroid moment tensor solutions are shown (except for Quepos 1924). The black star represents the global location of the 2002 Osa main shock from NEIC. QPl: Quepos Plateau. The green diamonds mark the positions of IODP CRISP-A drilling sites beneath the forearc.

mechanism, symptomatic of an event originating along the plate boundary fault. The Osa earthquake sequence includes two foreshocks and ~350 aftershocks during the ~15 days following the main shock. This event is the latest large earthquake sequence in the central Costa Rican seismogenic zone. It took place at the southeastern end of the seamount-covered segment, toward the western flank of the Cocos Ridge (Figure 1). Subduction of Cocos Ridge beneath Costa Rica uplifted a 135 km wide section of the continental slope seafloor that crests above sea level to form the Osa Peninsula. Northeast of Osa Peninsula, flat subduction of the ridge has been invoked to explain forearc shortening and coastal mountains formation, regional uplift, and Pleistocene decrease and termination of volcanic activity in the southeastern Costa Rica highlands [e.g., *Kolarsky et al*., 1995; *Fisher et al*., 2004; *Sitchler et al*., 2007]. Recent investigations show evidence of a subducting slab rather than flat subduction in southeastern Costa Rica [e.g., *Arroyo et al*., 2003; *Dzierma et al*., 2011; *Lücke*, 2012], and point toward a more complex tectonic history in this region, not entirely explained by the presence of the Cocos Ridge alone [*MacMillan et al*., 2004; *Morell et al*., 2012; *Vannucchi et al*., 2013].

The 2002 earthquake followed a 1999 Mw 6.9 megathrust earthquake to the northwest [*DeShon et al*., 2003] that nucleated along subducted relief of the Quepos Plateau and seamounts on the flank of the Cocos Ridge (Figure 1). It is speculated that subducted seamounts acted as an asperity in the 1999 earthquake [*Bilek et al*., 2003]. The main shock of the 2002 earthquake occurred farther up the flank of the Osa uplift, ~20 km southeast of the subducted relief. No subducting feature that may have been an asperity of the main shock is apparent. A local seafloor bulge over the main shock indicating a subducted seamount would

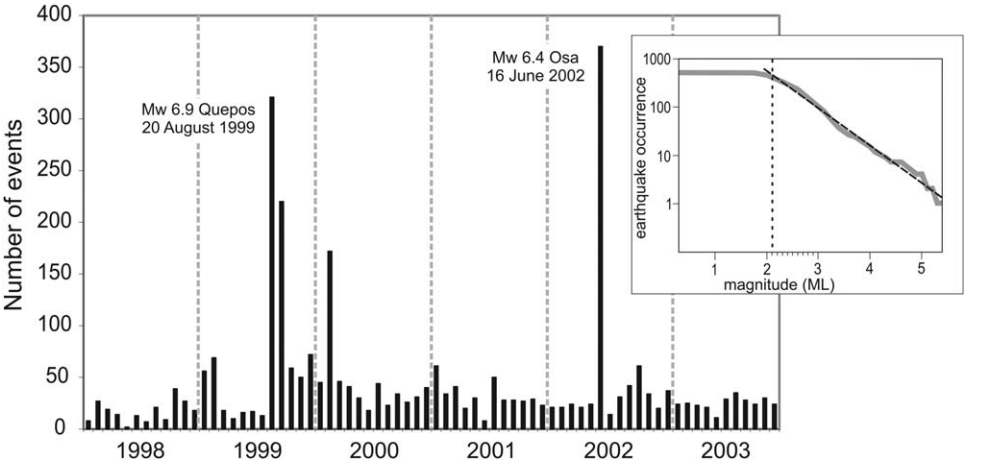

Figure 2. Number of earthquakes per month in the region offshore Quepos to Osa (Figure 1) from 1998 to 2003, according to the Red Sismologica Nacional (RSN) catalog (estimated completeness of mc ~3.3). The Osa sequence took place mainly during the last 2 weeks of June 2002. The inset presents the frequency—magnitude curve of the Quepos-Osa catalogue (estimated completeness of ML 2.1).

have low relief that could only be resolved in high-resolution bathymetry, but the main shock is not within the area of complete coverage mapped with multibeam bathymetry [*Kluesner et al*., 2013].

The source area of the 2002 Osa earthquake sequence is in the target area of the Costa Rica Seismogenesis Project (CRISP) from the Integrated Ocean Drilling Program (IODP). CRISP is the first scientific drilling project designed to sample plate boundary material at an erosional margin (Figure 1). The CRISP drilling proposal [*Vannucchi et al*., 2012; *Expedition 344 Scientists*, 2013] is focused on comparing samples from the stable and unstable segments of the plate interface. Since the uncertainties in locating earthquakes with distant global recordings make positions within either the assumed stable or unstable sliding regime uncertain, we revisited the 2002 Osa earthquake and its aftershocks using locally recorded earthquake data. Fortuitously, a nearby onshore-offshore passive seismic experiment was in progress during the earthquake (Figure 1). In addition, we conducted a moment tensor inversion for the main shock which supports the likelihood that the main shock nucleated at the plate boundary, in the vicinity of the CRISP IODP Site U1379 [*Vannucchi et al*., 2012].

Years of academic onshore and offshore investigations have characterized the area's regional geology and crustal structure. The area is optimal for drilling operations because of its low sediment supply, fast convergent rate, abundant seismicity, optimal weather conditions, and a shallow plate boundary [*Ranero et al*., 2007]. Depths to the seismogenic zone are suitable for drilling because subduction of the warm and thick hot spot ridge [*Sallarès et al*., 2003] fosters shallower than usual seismogenic plate coupling. It brings the seismogenic zone into scientific riser drilling depths. Here we report the analysis of a teleseismic waveform inversion and of seismological data from a local onshore-offshore array that indicates an earthquake asperity in the area proposed for sampling of a plate interface.

2. Data and Methods

A comparison of the seismic activity before and after 16 June 2002 shows that the Osa sequence lasted approximately 2 weeks (Figure 2). At the time, a temporary network of 15 short-period land stations and 23 ocean-bottom hydrophones (OBH) operated within the project SFB574 from the University of Kiel was deployed ~60–80 km west of the source area [*Arroyo et al*., 2009] (Figure 1). The availability of OBH records provided a unique opportunity to constrain earthquake locations much better than the usual location with global network data. We compiled a Quepos-Osa seismic catalog for the whole duration of the network operation, from April to the beginning of October 2002 (Figure 1). The data set incudes foreshocks, the main shock, and ~350 aftershocks of the Osa earthquake sequence between 16 and 30 June 2002. To further improve the event station coverage, readings from permanent stations in central and southeast Costa Rica of both, the Red Sismologica Nacional (RSN) and the Observatorio Sismologico y Vulcanologico de Costa Rica (OVSICORI) were incorporated in the data set (Figure 1). The final catalog encompasses a total of 48 local stations that recorded ~520 earthquakes within the Quepos-Osa area between April and October

2002. Apart from the main shock, local magnitudes range from 1.0 to 5.4, with an estimated catalog completeness of ML 2.1 (Figure 2).

Analyst-reviewed *P* wave arrival readings and initial locations were obtained using the program HYP [*Lienert and Havskov*, 1995] distributed with the software package SEISAN [*Ottemöller et al*., 2012]. The reading weighting scheme ranges from factor 0, corresponding to the lowest uncertainty (0.05 s), to factor 4 ($>$0.3 s) for doubtful readings that were not used. The total average *P* wave reading error is estimated at 0.13 s. Unfortunately, the only three-component stations available were those of the SFB574 land network, clustered in the northwest area of the seismometer array and the *S* wave arrivals are severely masked by other wave trains. Therefore, we use only *P* wave data in this study.

In addition, we used teleseismic data to further constrain the rupture process and the hypocentral parameters of the main shock. High-quality seismic waves were recorded by stations of the global broadband seismograph network, which enables a detailed characterization of the nucleating depth and rupture process using waveform inversion. Depth resolution results from the time separation between the direct *P* wave and the *pP* and *sP* phases; thus, waveforms are very sensitive to the time delay between the first arriving *P* wave and the later-arriving surface reflected phases. In this study, a sampling rate of 1 s is used. Thus, depth resolution is limited because the minimum depth increment resolved by depth phases *pP* and *sP* is, on the order, of 2 to 3 km [*Kikuchi and Ishida*, 1993].

2.1. Earthquake Relocation

Given its station-source distribution, we explored possible solutions by relocating the Osa catalog using two different velocity models. First, we obtained the minimum 1-D model by jointly inverting for velocity structure and hypocenter parameters [*Kissling et al*., 1994]. Second, we constructed a 3-D model based on the wide-angle records analyzed offshore by *Ye et al*. [1996], *Stavenhagen et al*. [1998], *Walther* [2003], and *Sallarès et al*. [2003]; the minimimum 1-D model for Costa Rica from *Quintero and Kissling* [2001]; and the slab and Moho geometry from *Lücke* [2012] and *Arroyo et al*. [2013]. We then used the nonlinear probabilistic approach [*Moser et al*., 1992; *Tarantola and Valette*, 1982] coded in the program NonLinLoc [*Lomax et al*., 2000], in order to explore the associated uncertainties.

2.1.1. Minimum 1-D P Wave Velocity Model

We used the VELEST algorithm to derive the minimum 1-D *P* wave velocity model [*Kissling et al*., 1994] for the Osa catalog. The selected data set includes $\sim$90 earthquakes with an azimuthal gap $\leq 180^{\circ}$ and at least 12 *P* wave arrivals with reading uncertainty $\leq$ 0.1 s. Because this reduced data set prevented the estimation of a stable model, we also included background seismicity recorded from April to October 2002. To sample the velocity structure closer to the trench, where the main shock and first aftershocks occurred, we used events with a gap $\leq 210^{\circ}$ and with at least 15 observations for the inversions. These criteria define a final data set of 191 events with a total of 3843 *P* wave arrivals (Figure 3a).

The VELEST ray tracer assumes that all the stations are located within the first model layer. The Osa catalog includes stations located from the trench to the volcanic arc, which means a 7 km thick first layer with a constant velocity. This layer prevents inversion convergence and is rather unrealistic because near-surface velocities exhibit a strong gradient. We therefore neglected station elevations during the inversions, and their effect is included in the resulting station corrections (Figure 3b).

Good convergence was found between 10 and 35 km depth (Figure 3b). High and low-velocity tests allowed us to investigate the dependence of the solution on the initial model, confirming that the number and distribution of hypocenters shallower than 10 km and deeper than 35 km were not favorable to resolve the shallowest and deepest layers. The velocities for the first 10 km are based on a wide-angle model by *Stavenhagen et al*. [1998], which crosses the Osa-Quepos region (Figure 1), and on the direct measurements from CRISP-A for the first kilometer drilled (Site U1379) [*Expedition 334 Scientists*, 2011], and were overdamped during the inversions. The corresponding station corrections (Figure 3b) present a pattern clearly related to the geological setting, the geometrical configuration of the network, and the effects of station elevations. The final RMS for the data set is 0.15 s.

We conducted stability tests [*Haslinger et al*., 1999] with randomly and systematically shifted hypocenter locations, and with both, fixed and floating models, to investigate the robustness of the minimum 1-D model. The random hypocenter shift had a maximum value of 10 km in any direction. During the random

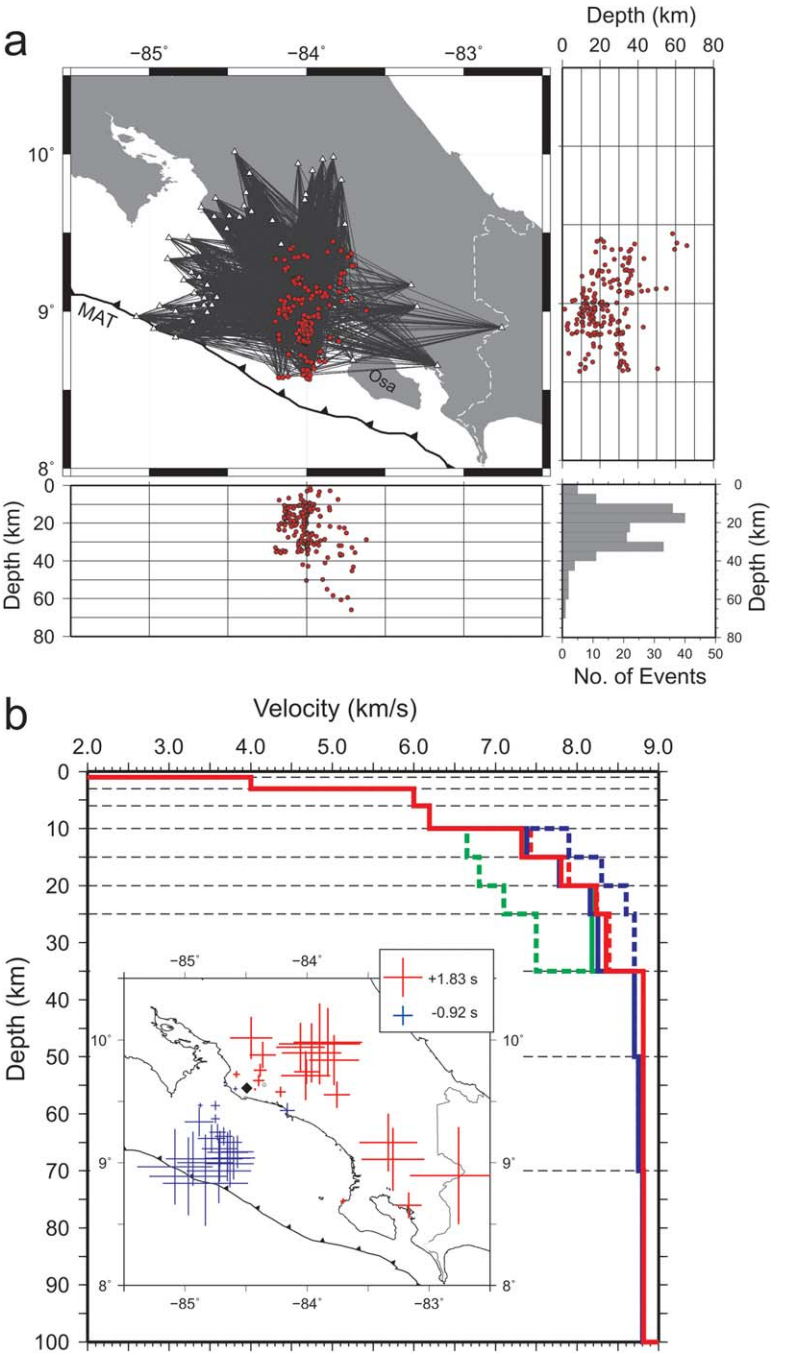

Figure 3. (a) Distribution of 191 hypocenters selected for determination of the *P* wave minimum 1-D model, in map view and vertical cross sections in east-west and north-south directions. Starting locations estimated using the 1-D model for Costa Rica from *Quintero and Kissling* [2001]. The triangles represent stations. The black lines show raypaths between epicenters and stations. (b) Final velocity model (red bold line) and station corrections for the minimum 1-D model (inset). The reference station is marked by a diamond. The high (blue lines) and low-velocity (green lines) tests are shown (the dotted lines are starting models, the bold lines are the models after inversion). The axis of the Middle America Trench is indicated by a toothed line.

tests, we observed a very good retrieval of epicenters and a moderate recovery of focal depths, where ~90% of the foci had a depth difference smaller than 5 km with those estimated by the inversion with the real data. The systematic tests showed only 20–30% hypocenter recovery with depth differences smaller than 5 km. These results indicate a good degree of independence between epicenters and velocity structure, and a substantial coupling between the velocity and the depths/origin times.

2.1.2. Nonlinear Probabilistic Relocation

This approach relies on the use of normalized and unnormalized probability density functions to express the available knowledge regarding the parameter values. When the density functions, given the a priori information on the model parameters and on the observations, are independent and the theoretical relationship can be expressed as a conditional density function, a complete, probabilistic solution can be expressed as an a posteriori density function (PDF) [*Tarantola and Valette*, 1982]. The final hypocenter locations correspond to the maximum likelihood value, i.e., the minimum misfit point of the complete PDF. We used the Oct-Tree importance sampling algorithm, which provides an accurate and complete mapping of the location PDF using recursive subdivision and sampling of cells in 3-D space to generate a cascade of sampled cells. The density of sampled cells follows the PDF values of the cell center leading to a higher density of cells in the areas of higher PDF (A. Lomax and A. Curtis, Oct_tree importance sampling algorithm, available at http://alomax.free.fr/nlloc/, 2014).

The PDF solution includes location uncertainties due to the spatial relation between the network and the event measurement error in the observed arrival times, and errors in the calculation of theoretical travel times. NonLinLoc also provides traditional Gaussian estimates, including the expectation hypocenter location and the 68% confidence ellipsoid. We follow a scheme similar to that used by *Husen and Smith* [2004] to classify the earthquake location quality. Examination of numerous scatterplots allowed us to define four quality classes based on final RMS, distance between maximum likelihood and expectation hypocenter locations, and the average of the 68% confidence ellipsoid axes.

Earthquakes with RMS errors larger than 0.5 s belong to class D and are not used in this study. Events with location quality A show a well-defined PDF, a difference between maximum likelihood and expectation hypocenters of 2 km and lower, and maximum average of ellipsoid axes of 5 km. The same hypocenter estimation differences but averages for the ellipsoid axes higher than 5 km define quality B. Their epicenters and focal depths are still relatively well defined. Earthquakes with differences in hypocenter estimations higher than 2 km are classified as C, showing relatively well-defined epicenters but higher uncertainty in depth.

2.2. Moment Tensor Inversion and Source Time Function

We used an iterative least squares inversion [e.g., *Kikuchi and Kanamori*, 1991] of azimuthally distributed seismic *P* and *SH* body-wave signals from stations at distances of about 30°–90°, yielding the rupture mechanism, depth, and source time function. Waveforms are corrected for instrument responses to obtain displacement seismograms. The inversion assumes attenuation with a t^* (travel time divided by average Q) of 1 s for *P* waves and 4 s for *SH* waves. The Green's functions were computed for simple layered source and receiver structures connected by geometric spreading for a deeper ak135 Earth model [*Kennett et al*., 1995]. The velocity structure at the source included a water layer overlying a half space with Vp = 6.0 km/s, Vs = 3.55 km/s, and ρ = 2.67 g/cm^3. The source was fixed at the epicenter, determined from the local and regional data described above.

For the inversion, we chose 15 *P* waves and 6 *SH* waves that provided good quality waveforms (Figure 4). The mechanism indicates shallow underthrusting with a strike = 112°, dip = 83°, and rake = 84°, occurring shallower than 10 km with a best fit centroid depth of 6 km. Thus, the mechanism is very similar to the gCMT solution: strike = 112°, a dip of 77°, and a rake of 87° (conjugate plane: strike = 303°, dip = 13°, rake = 101°), but much shallower than the gCMT centroid of 15 km. Figure 4 shows the waveform inversion with the waveform fit and centroid depth. The best depth estimates indicate that most of the seismic energy was radiated at shallow depth below the continental slope.

In addition, we surveyed trade-offs between the velocity-depth profile at the source location and depth. We also run the inversion replacing the half space model by both the minimum-1-D model and the 3-D model sampled at the epicenter. However, results are very similar, favoring a centroid depth of less than 8 km. Further, to test possible trade-offs between centroid depth and fault dip, we fixed the strike and rake and performed a grid search with the fault dip ranging from 3° to 32° and the centroid depth ranging from 2 to 24 km. The grid search supports the results from the inversion, with two minima at 6 km (dip 6°) and 8 km (dip 11°) depth. Solutions with smaller dip and shallower depth provided much lower misfits than solutions with larger depth (>10 km) and dip (>12°).

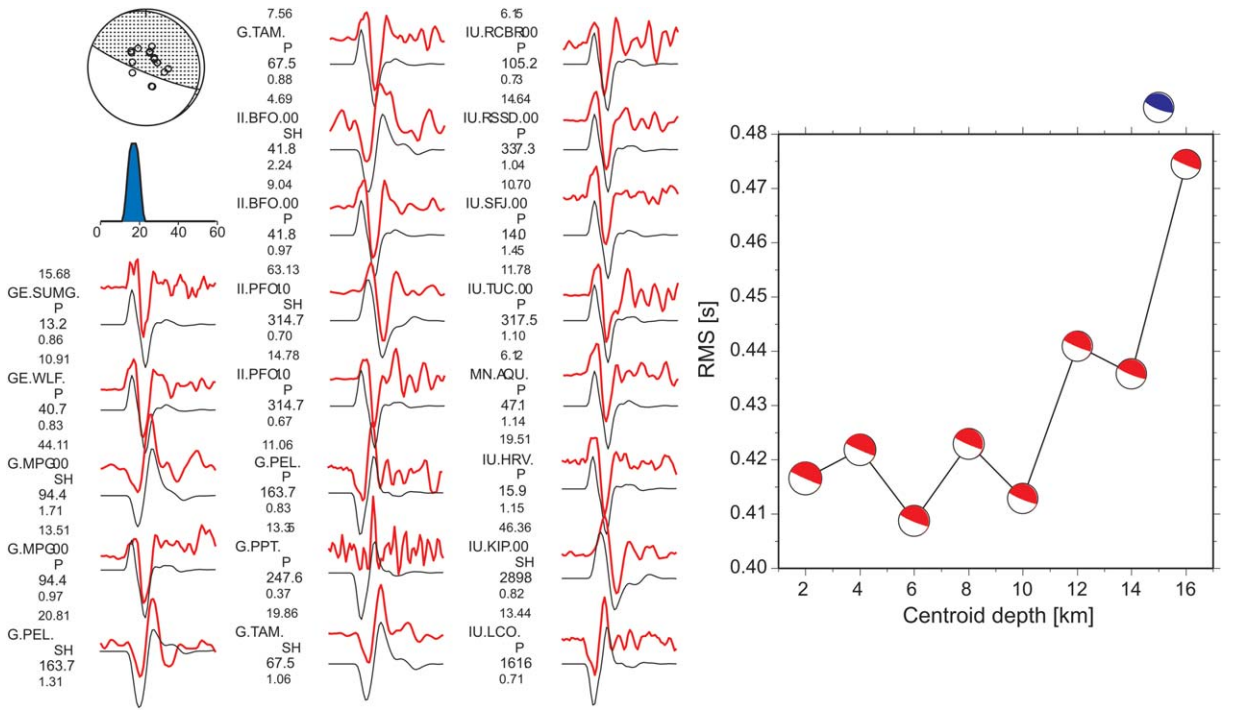

Figure 4. Waveform inversion using global GSN stations at distances of 30°–90°, with waveform fit and centroid depth. The best depth estimates indicate that most of the seismic energy was radiated at shallow depth below the continental slope. This supports the nucleation of the Osa earthquake at a depth of 6–10 km near CRISP IODP Site U1379.

3. Results and Discussion

3.1. Preferred Relocation

Figure 5 shows the relocation of the Osa earthquake sequence with NonLinLoc using both, the 1-D and the 3-D velocity models. The oceanic and continental Moho reflectors and the slab top from the model of *Stavenhagen et al.* [1998] have been added for reference in the cross section down to ~25 km depth. We adjusted the slab top geometry under the coast to account for the intraslab seismicity relocated in the tomographic model of *Husen et al.* [2003] and the slab structure proposed by *Lücke* [2012] and *Arroyo et al.* [2013].

The 3-D model encompasses structural a priori information to simulate the complex structure of the subduction zone, including, for example, the eastward-thickening crust of the Cocos Ridge [*Walther*, 2003], changes in the slab dip angle beneath central and south Costa Rica [*Arroyo et al.*, 2013; *Lücke*, 2012], and an uplifted forearc in south Costa Rica [*Sak et al.*, 2009]. We tested several reasonable velocity and geometrical variations of the model to explore structural effects on earthquake relocation. On average, the relocations using the preferred 3-D model are shifted 6.8 km to the west and 2.3 km shallower than those using the minimum 1-D model. For both models, earthquakes in quality class A show average RMS of 0.13–0.14 s and mean focal uncertainties between 3 and 4 km. For class B, those values range from 0.14 to 0.15 s and 7 to 8 km, and 0.14 and 0.15 s and 8 to 10 km for class C, respectively. The average RMS residuals are comparable to the estimated reading error of the data set (0.13 s).

In general, the average relocation RMS using different versions of the 3-D model increases to values of 0.20–0.28 s when station corrections are not used; when station delays are included, the RMS values do not vary significantly with changes in the model (0.14–0.17 s). High velocities (> 6.0 km/s) at shallow depths (5–10 km) in southeast Costa Rica increase the average westward shift of the locations up to ~10 km. We prefer lower velocities in that region, corresponding to an uplifted forearc. With the 3-D model, the foci tend to be shallower than the estimations made using the 1-D model, but the average depth shift remains under 4 km (shallower) even when important changes in the model such as a thickened, low-velocity (6.3–6.9 km/s) oceanic crust under southeast Costa Rica are contemplated. Throughout all model modifications, the average difference in latitude remains under 2.2 km.

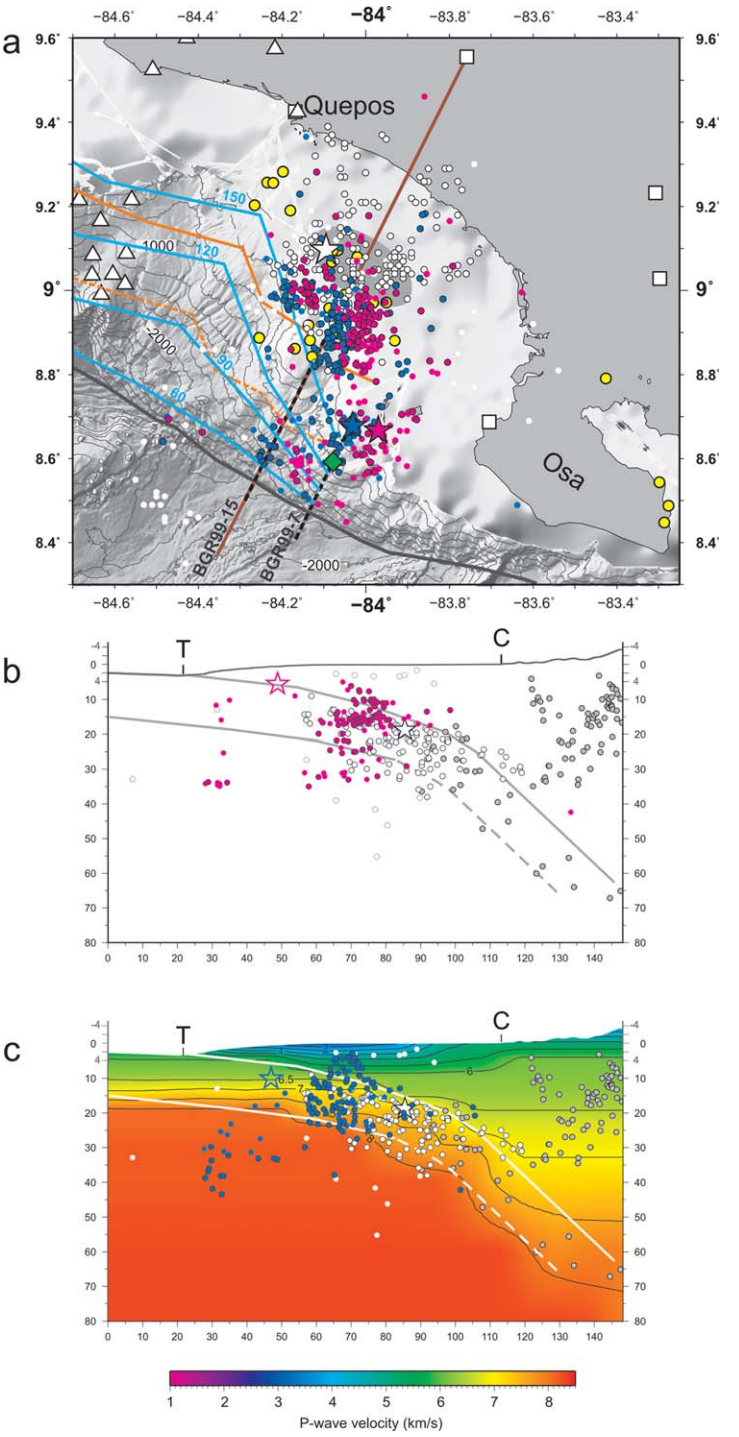

Figure 5. (a) Probabilistic earthquake relocation of the 2002 Osa earthquake sequence, using the minimum 1-D model (magenta circles) and the a priori 3-D model (blue circles). Only events recorded between 16 and 30 June (i.e., the Osa sequence) by at least eight stations are shown. Open circles represent events with location quality C. The main shock relocations (stars) are shown with the corresponding colors. White triangles and squares represent seismic stations. The white circles are the 1999 Quepos aftershocks relocated by *DeShon et al.* [2003]; the 1999 main shock is shown according to relocation by the RSN. The rupture of the 1999 Quepos earthquake is shown as a dark gray area [*Bilek et al.*, 2003]. The solid blue lines represent the isotherms along the plate boundary after *Ranero et al.* [2008] as labeled (in °C). The solid orange line is the 100°C isotherm according to *Harris et al.* [2010]; the dashed orange line is its uncertainty. The yellow circles are earthquakes with magnitude between 5 and 6 (Mw) occurred from 1992 to 2013 (relocation with local RSN stations, this study). The black dashed lines are reflection lines as indicated (shown in Figure 8). The green diamonds mark the positions of CRISP-A drilling sites (U1379 lays beneath the blue star). The solid gray line marks the MAT axis. Seismicity cross section showing only (b) 1-D and (c) 3-D relocations. The cross-section orientation coincides with line BGR-15, extended inland (brown line). Hypocenters projected from 10 km to each side of the profile. Gray circles (not shown in Figure 5a) are earthquakes from the tomography data set by *Husen et al.* [2003]. Slab geometry from *Stavenhagen et al.* [1998], *Arroyo et al.* [2013], and *Lücke* [2012]. T marks the trench axis and C marks the coast positions.

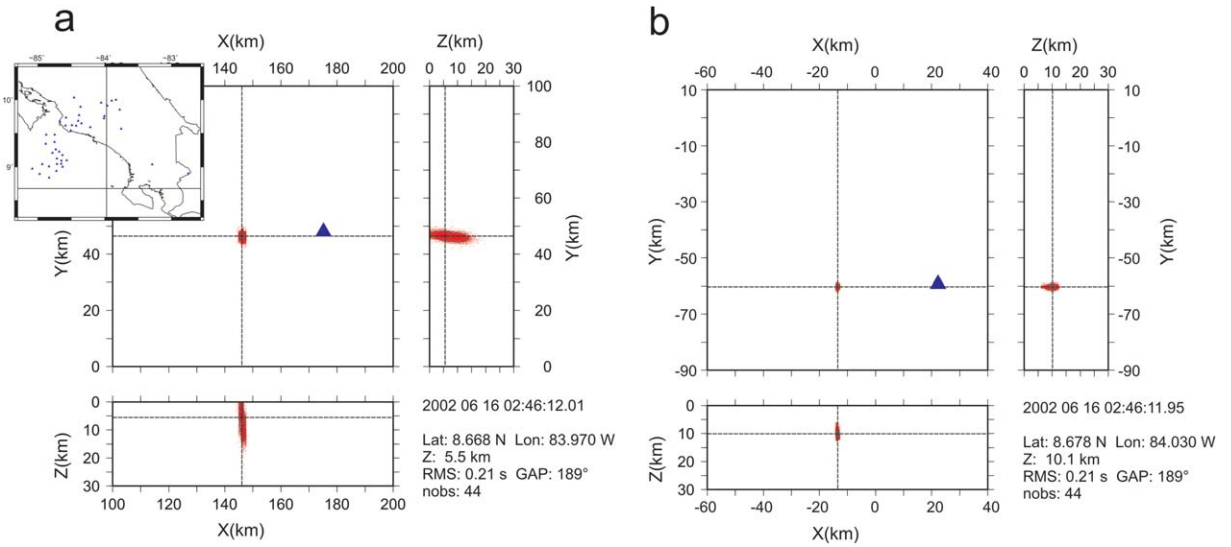

Figure 6. Density scatterplots for the Osa main shock in plane view in x-y direction and cross sections in x-z and y-z directions, using (a) the minimum 1-D model and (b) the 3-D model. The intersections of the dashed lines mark the maximum likelihood hypocenter location. Open circles denote expectation hypocenter location. Projection of the 68% confidence ellipsoid is shown by gray lines. The insets include all the seismological stations (triangles) used to locate the event (intersection of bold lines). Nobs: number of observations.

The relocation differences resulting from using the different models could be attributed to several factors, in addition to the obvious differences between the 1-D and 3-D velocity models. First, the velocities in southeastern Costa Rica are not well known because of the lack of extensive active seismic or tomographic experiments. Further, although this is the best available local data set for the Osa sequence, the station distribution is asymmetrical, with most stations located west of the sequence (Figure 3a). The lack of stations situated closer ($<$30 km) to the source areas hinders an optimal depth control due to the trade-off between depth and origin time. In addition, well-determined *S* wave arrivals may improve and constrain depth determinations [*Gomberg et al*., 1990] but are not available for this data set.

The comparison of the relocations using the minimum 1-D model and those obtained using the a priori 3-D velocity model indicates that the location of the main shock and aftershocks is not extremely influenced by lateral velocity heterogeneities. A minimum 1-D model is the velocity model with station corrections that most closely reflects the a priori information obtained by other studies, but at the same time leads to a minimum RMS of travel time residuals for all earthquakes. Therefore, in the following, we will use the relocations from the minimum 1-D model for the interpretation of the tectonic activity of the area.

3.2. Main Shock Nucleation

The relocation of the main shock with the 1-D model places the most likely hypocenter at 5.5 km depth, whereas within the preferred 3-D model it is located at $\sim$10 km depth and $\sim$6 km further west. Figure 6 presents the density scatterplots for both hypocenter locations. As expected from the station distribution, the epicenter location is well constrained but the vertical uncertainty is clearly greater. On the other hand, the best fit for the moment tensor inversion occurs at 6 km depth, with another local minimum at 10 km depth, also suggesting a shallow origin (Figure 4). Furthermore, the solutions indicate a plane dipping at $\sim$7°, in close agreement with the dip angle in this portion of the plate interface as imaged in the wide-angle model from *Stavenhagen et al.* [1998]. Projected on the depth images of MCS lines BGR99-7 and BGR99-15 (Figure 7), the main shock maps on the location of the reflection of the plate boundary, indicating also that was generated by slip on the main fault zone. Altogether, our data suggest that the main shock nucleated at the plate boundary, near CRISP IODP Site U1379 (Figures 5 and 7).

The Mw 6.4 main shock has a well-defined thrust fault mechanism (Figures 1 and 4) and occurs at a location that is slightly shallower and $\sim$10 km closer to the trench compared to other thrust earthquakes with magnitudes Mw greater than 5 in the Central Pacific region in Costa Rica (Figure 5a). It occurred 30–40 km seaward of previous large (M $>$ 6) events, typical for the northwest of the study area. This seaward anomalous

location seems to indicate an along-strike variation in the mechanical coupling along the subduction zone from north and central Costa Rica toward the Osa region. The variation corresponds to a major change in the geological structure of the subduction zone. The Osa event is located roughly under the shelf edge which in this region extends several tens of kilometers seaward compared to the northern and central Pacific margin in Costa Rica. In addition, it is located where the thick and buoyant crust of the Cocos Ridge is underthrusting the margin. Several interplate earthquakes with magnitude Mw up to 5.7 have also occurred under the Osa Peninsula, southeastward from the 2002 main shock and at similar distances from the trench (Figure 5a).

3.3. Aftershock Sequence Distribution

Despite model and relocation differences, the seismicity shows a remarkably similar pattern (Figures 5 and 8): a cluster around and landward of the main shock, and two clusters roughly colocated with those observed for the 1999 Quepos earthquake aftershocks [*DeShon et al*., 2003], but extending a few kilometers further updip. The 1999 Quepos sequence has been associated with rupture of lower plate relief probably related to the subducted Quepos Plateau and associated seamounts [*Bilek et al*., 2003]. A fourth small cluster occurred between 20 and 21 June, west of the main shock and closer to the trench.

The depth distribution suggests that most earthquakes with epicenters ~40 km and further from the trench originated at the plate interface or in the oceanic crust (Figures 5b and 5c). The events closer to the trench show focal depths ranging from a few kilometers down to ~40 km depth (Figures 5b and 5c). These deep foci indicate origins in the entire oceanic crust and the upper mantle. Intracrustal seismic activity in this area has also been revealed by the relocation of the 1999 Quepos aftershocks [*DeShon et al*., 2003] and a tomographic model [*Dinc et al*., 2010]. The subduction of thickened crust associated with the Cocos Ridge begins in the vicinity of the Quepos Plateau (Figure 1). The intraplate seismicity seems to be caused by increased internal deformation in the thickened crust where the subduction angle steepens (Figure 4).

The aftershock sequence of the 2002 event displays several interesting characteristics, including the spatial distribution of its temporal evolution, and the uneven spatial extend of the aftershocks from the main shock location. Figure 8 shows the spatial distribution of the time evolution of the 2002 Osa sequence. It started with two foreshocks (ML 4.8). The first one occurred on 7 June around the updip limit of the 1999 Quepos sequence and the second one, less than 10 km landward of the Osa main shock and 3 days in advance. The main shock occurred at 02:46 UTC on 16 June. During the next ~13 h, the aftershocks surrounded it but most of them seemed to have originated deeper in the Cocos Plate (Figure 8). Although some seismicity still occurred in the vicinity of the main shock, later activity migrated northwestward, and concentrated in the region of the 1999 Quepos aftershocks.

Modeling of the Coulomb stress changes caused by the 1999 Quepos earthquake [*Bilek and Lithgow-Bertelloni*, 2005] does not suggest a correlation with the 2002 Osa earthquake. Those authors mention the possibility that viscoelastic relaxation may have played a role in triggering the Osa sequence. The Osa main shock could have also been triggered by strain accumulation at the edge of 1999 activity, where the foreshocks originated. In effect, most aftershocks following the 2002 main shock within 2 weeks are located possibly outside of the region of its coseismic rupture, in the zone updip of the 1999 sequence, which may have been a conditionally unstable region (Figure 8). Thus, it appears that they do not inform about the coseismic rupture area but delineate the region that was conditionally unstable for these stresses.

The boundary to the southeast and to the northwest of the aftershock distribution may however indicate different characteristics along the plate boundary. The lack of aftershocks under the continental slope toward the northwest (Figures 1 and 9) may be due to a change in mechanical coupling along the fault zone, into an area of unstable slip. Whereas the abrupt termination toward the southeast, under the continental shelf of the Osa Peninsula, may actually indicate that coupling there is high and that stresses did not overcome the yield stress and the region remains strongly coupled. This is the rupture region of the 1983 Mw 7.4 Golfito earthquake (Figure 1), which is probably still accumulating deformation leading to a possible rupture in the near future.

An interesting feature of the aftershock distribution is the large number of events seaward of the main shock that occur below the plate boundary fault, within the oceanic crust and uppermost mantle. A similar occurrence followed the Mw 7.6 tsunamigenic earthquake off Java in 1994 [*Abercrombie et al*., 2001]. Like

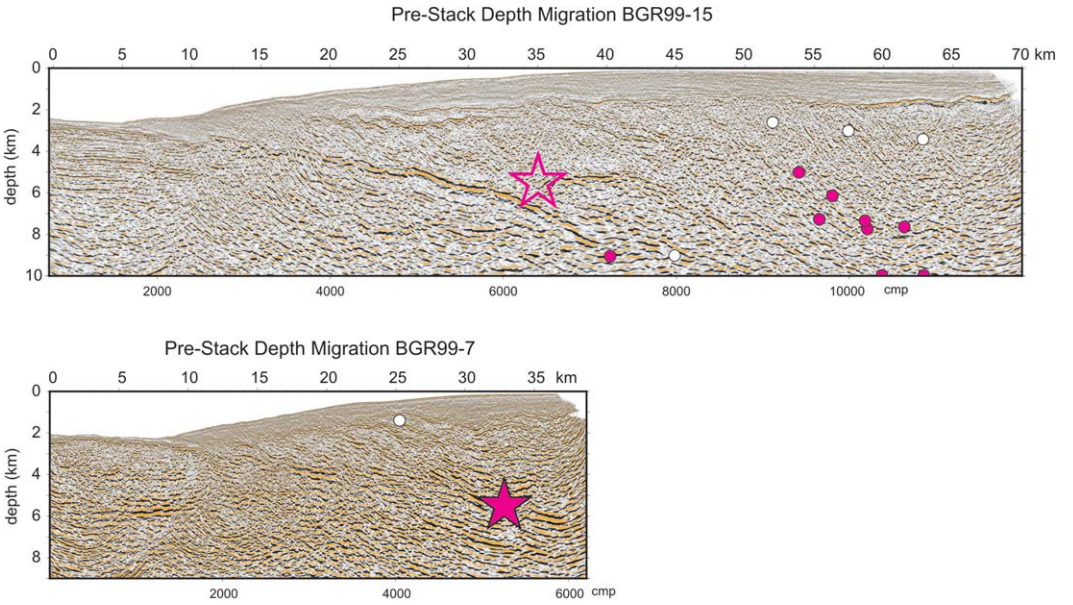

Figure 7. Seismic depth images (prestack depth migration) crossing the 2002 Osa sequence area. Minimum 1-D model relocations (magenta circles and stars) are superimposed. The profile locations are indicated in Figures 5a and 8a. The open star is the projection of the Osa main shock, which was generated ~20 km southwest from profile BGR99-15. The main shock relocation (closed star) nearly collocates with the reflection of the plate boundary fault. Together with the teleseismic waveform inversion, the data suggest that it was generated at the plate boundary (Figure 5).

the Osa earthquake, the 1994 tsunamigenic earthquake nucleated close to the trench axis. The main shock was a shallow underthrust event. However, most aftershocks had normal fault mechanisms and were interpreted to have occurred in the subducting oceanic plate in response to the change in stress caused by slip over a subducting seamount. The relief of the Cocos Ridge on the subducting plate may have had a similar effect, explaining the earthquakes originating deep in the subducting plate near to the trench axis.

3.4. Comparison of Structure and Seismic Activity

A good correlation has been observed between the onset of seismicity and temperatures of 150°C along the subduction megathrust [*Hyndman et al*., 1995, *Oleskevich et al*., 1999], which suggests that the transition from stable sliding to stick-slip behavior is determined by temperature-controlled reactions in the subducted sediments. Pressure and temperature-dependent processes that take place below 100°–150°C, such as porosity reduction, fault zone cementation, dewatering, and consolidation, are invoked to explain the start of the interplate seismicity in accretionary margins [*Moore and Saffer*, 2001; *Moore et al*., 2007]. The combined effect of this diagenetic and low-grade metamorphic reactions increases the effective stress and coupling at the plate boundary, and strengthens the overriding plate allowing the storage of elastic energy released during earthquakes.

Two thermal models are available for the southern end of the Middle America Trench (Figure 9). *Ranero et al*. [2008] use a detailed thermal conductivity model of sediments and basement, and the depth to the plate boundary based on seismic structure to estimate the temperature along the shallower part (<20 km) of the plate boundary in several transects from Nicaragua to the Osa Peninsula. *Harris et al*. [2010] use finite element thermal models of the Pacific margin of Costa Rica, incorporating simulations of fluid flow within the subducting aquifer and plate convergence effects. Their models are constrained at the margin front with the same heat flow data set presented by *Ranero et al*. [2008], but are derived with a rougher overall margin-wedge geometry.

Along the northern and central Costa Rica Pacific margin, the beginning of interseismic interplate seismicity has been observed at around 15 km depth [*DeShon et al*., 2006; *Arroyo et al*., 2013]. In central Costa Rica, this nearly follows the edge of the continental platform (Figure 9) and temperatures of 120°–150°C along the plate boundary, depending on the thermal model used for comparison. But under the continental shelf and slope offshore the Osa Peninsula, our data indicate that the nucleation of a relatively large event

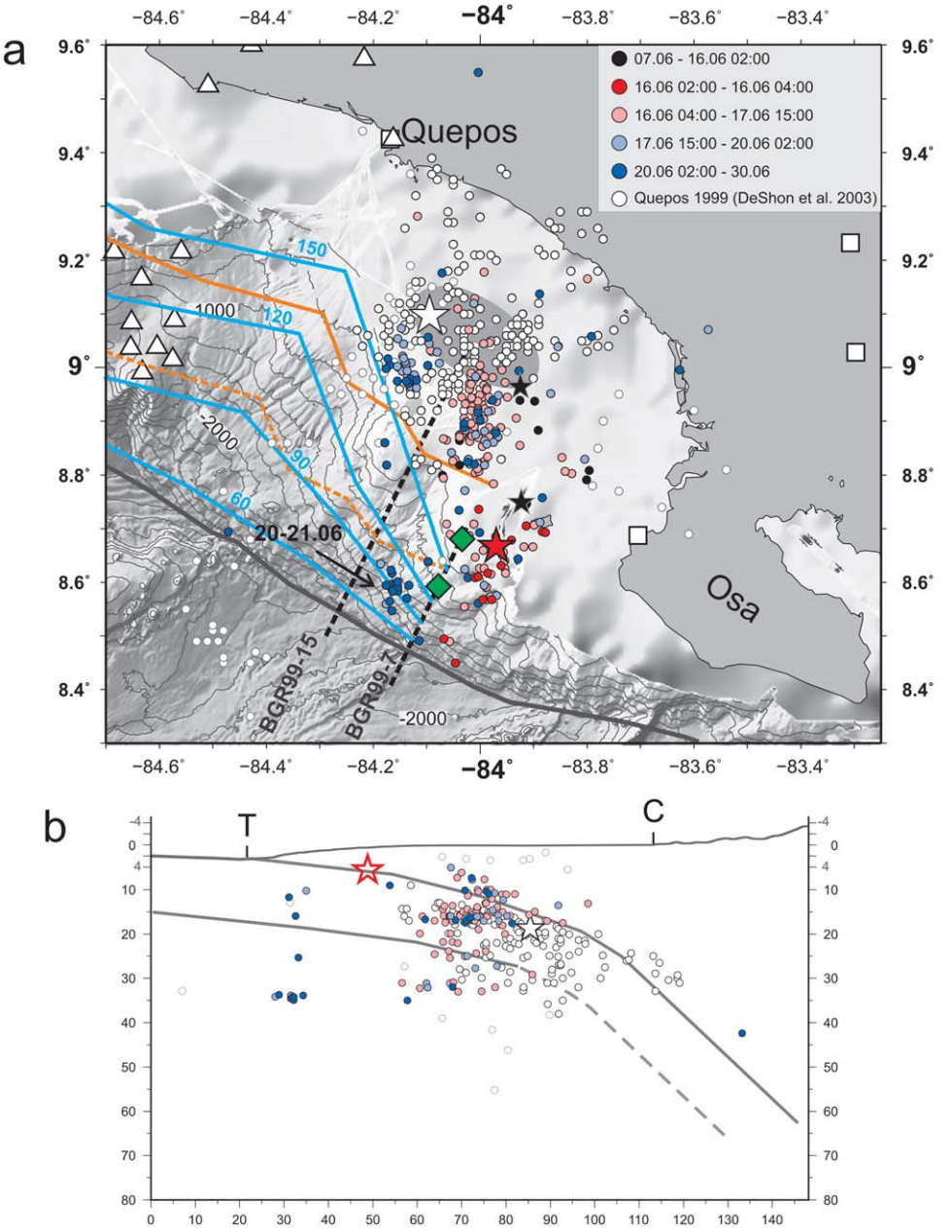

Figure 8. Spatial distribution of the 2002 Osa sequence temporal evolution, as indicated in the map inset. The relocations are from the minimum 1-D model. Other features are shown as in Figure 5. During the first hour, the seismicity surrounded the main shock but most of it seemed to have originated deeper in the Cocos Plate. In the following 2 weeks, although some seismicity still occurred in the vicinity of the main shock, the activity migrated northwestward, and overlapped the area of the 1999 Quepos aftershocks.

occurred possibly as shallow as 6 km. There, temperatures of 120°C–150°C have been estimated by *Ranero et al*. [2008] and less than 100°C by *Harris et al*. [2010], or ~100°C when frictional heating is allowed into their models (Figures 5a and 9).

Based on geophysical, geochemical, and geological data collected mostly along the Middle America Trench offshore Nicaragua and Costa Rica, *Ranero et al*. [2008] propose that a decrease in fluid abundance along the plate boundary fault marks the progression from stable to unstable slip at all types of subduction margins. Following their model, the 2002 Osa sequence originated where most of the overpressured fluids liberated from subducted sediments at shallower depth and temperatures of 50–160°C have escaped upward through fractures in the overlying plate. The diminishing of overpressured fluids at the fault zone allows an

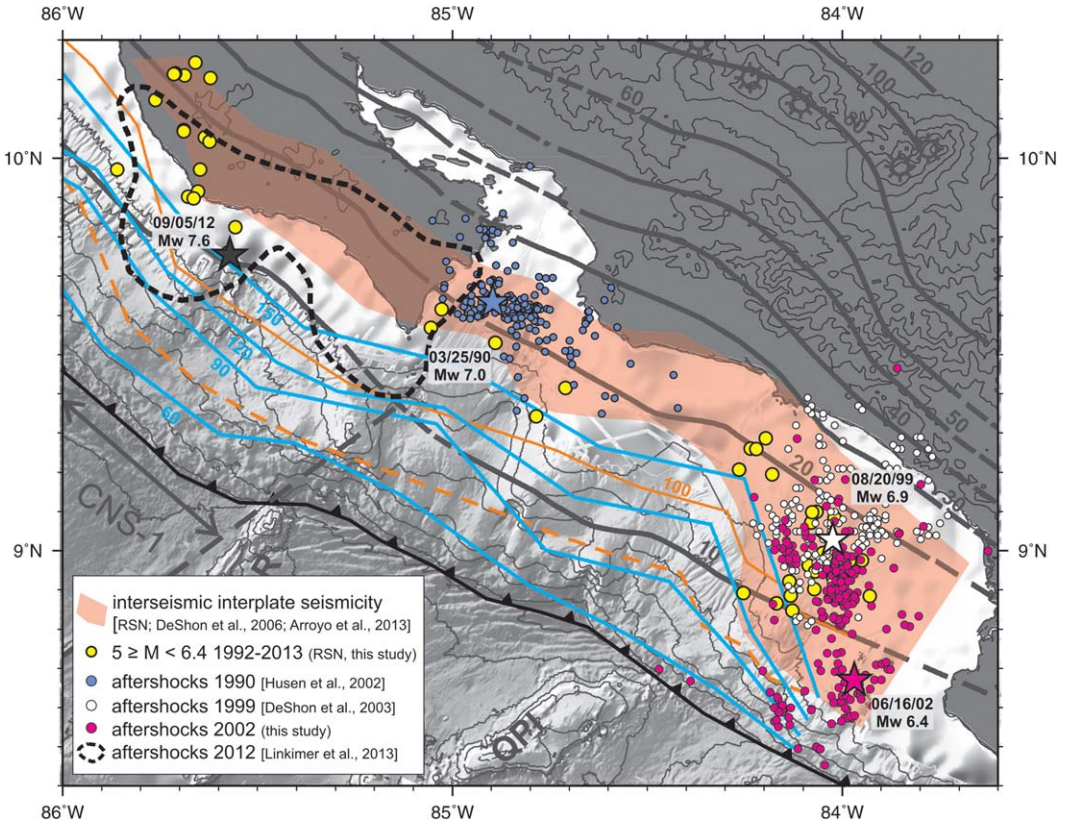

Figure 9. The 2002 Osa sequence presented in the context of the Costa Rican megathrust seismogenic zone. The interseismic interplate seismicity (red shadow) recorded in Costa Rica by "amphibian" and local permanent seismological networks, and recent large earthquakes (Mw > 6.0) and its aftershocks are shown. The yellow circles are earthquakes with magnitude between 5 and 6 (Mw) that occurred offshore Costa Rica from 1992 to 2013 (relocation with local RSN stations, this study). The solid blue lines represent the isotherms along the plate boundary after *Ranero et al.* [2008] as labeled (in °C). The solid orange line is the 100°C isotherm according to *Harris et al.* [2010]; the dashed orange line is its uncertainty. Along the Costa Rican Pacific margin, the beginning of interseismic interplate seismicity closely follows the edge of the continental platform. In central Costa Rica, the aftershock and rupture areas of recent large earthquakes (Mw ~7) have been contained within the area of interseismic interplate seismicity. Here the onset of the seismogenic behavior occurs at ~15 km depth, but toward the Osa Peninsula it seems to start at less than 10 km depth. This is probably caused by the relative high temperatures of the subducting oceanic crust and the proximity of the Cocos Ridge, which might accelerate the processes involved in seismogenesis [*Ranero et al.*, 2008].

increase in grain-to-grain contact and thus in effective stress on the fault. This augmented stress may be responsible for an increased mechanical coupling, enabling the transition from stable to unstable seismic behavior along the plate interface. Simultaneously, the upper plate thickens and gains strength. At the Osa main shock location, the relative high temperatures of the subducting oceanic crust and the proximity of the Cocos Ridge might accelerate the processes involved in seismogenesis [*Ranero et al.*, 2007]. Furthermore, the subduction erosion rates estimated by *Vannucchi et al.* [2013] at IODP Site U1379 imply rapid upward migration of the plate interface in the low-friction regime of the forearc. This influences the geometry and the properties of the interplate seismogenic zone and could propitiate anomalous stresses and earthquake rupture characteristics there [*Vannucchi et al.*, 2013].

The rupture process of the 2011 Mw 9.0 Tohoku Earthquake in northeast Japan showed widespread areas of large coseismic slip (~50 m) near the trench axis [e.g., *Fujiwara et al.*, 2011; *Yue and Lay*, 2013], apparently challenging the concept of stable sliding in the shallowest part of the megathrust. *Loveless and Meade* [2011] point out that it is still an open question if the slip under the outermost forearc can be caused by dynamic overshoot [*Ide et al.*, 2011] or is the result of strain accumulation during the interseismic period of the seismic cycle. Offshore of Central America, IODP drilling may help to answer some of the fundamental questions, as the Costa Rica Seismogenesis Project (CRISP) is designed to explore the processes involved in the nucleation of large interplate earthquakes at tectonically erosional subduction zones. Our analysis of the 2002 Mw 6.4 Osa earthquake strongly supports the notion that CRISP will be able to reach the seismogenic zone.

4. Conclusions

A temporary network of OBH and land seismometers recorded the 2002 Mw 6.4 earthquake 30 km west of the Osa Peninsula. The temporary network records were combined with those from permanent land stations of the local networks to relocate hypocenters. Most of the catalog has an azimuthal coverage of 180° or better, providing constraints unusual for location of most offshore earthquakes and their aftershock sequences. We successfully relocated the Osa catalog using a probabilistic approach within a minimum 1-D *P* wave velocity model derived during this study and a 3-D *P* wave velocity model based on previous seismic works.

The preferred relocation of the main shock places it ~25 km from the trench, at ~5–10 km depth, in the vicinity of CRISP IODP Site U1379. This relocation is constrained to <5 km in the horizontal and < 15 km vertically. The teleseismic waveform inversion performed in this study indicates a shallow underthrusting mechanism, with a best fit centroid depth of 6 km. Most of the seismic energy was generated at shallow depth below the continental slope, in good agreement with the earthquake relocation and the plate interface position imaged by previous, depth-migrated seismic data.

The aftershocks were concentrated around the main shock during the next ~13 h. Much of this activity originated in the oceanic crust and mantle. In the days following the main shock, aftershocks overlapped and extended a few kilometers updip of the 1999 Quepos aftershock area. The Osa aftershock sequence occurred where interplate temperatures are ~100°C or 150°C, depending on the thermal model used for comparison and considerably shallower than in northern and central Costa Rica. This observations suggest that the hotter and buoyant crust of the Cocos Ridge has brought seismogenic processes to shallower depth than typically elsewhere.

Acknowledgments

The seismic waveforms from the SFB network used for this paper are available upon request from the main author. The RSN and OVSICORI waveforms can be requested directly from their staff. We thank L. Linkimer, C. Redondo, and F. Vega from RSN and OVSICORI for making their data available. S. Husen for valuable suggestions during modeling. C. Leandro and G. E. Alvarado are thanked for *P* wave velocity measurements in local geological formations. We thank two anonymous reviewers and Associate Editor Paola Vannucchi for thoughtful comments that greatly improved the manuscript. Most of the figures were generated with GMT [*Wessel and Smith*, 1998]. This work was supported by DFG grant GR1964/17-1 and by former project SFB574.

References

Abercrombie, R. E., M. Antolik, K. Felzer, and G. Ekström (2001), The 1994 Java tsunami earthquake: Slip over a subducting seamount, *J. Geophys. Res.*, *106*(B4), 6595–6607, doi:10.1029/2000JB900403.

Adamek, S., F. Tajima, and D. A. Wiens (1987), Seismic rupture associated with subduction of the Cocos Ridge, *Tectonics*, *6*(6), 757–774, doi:10.1029/TC006i006p00757.

Arroyo, I., S. Husen, and E. Flueh (2013), The seismogenic zone in the Central Costa Rican Pacific margin: High-quality hypocentres from an amphibious network, Eos Trans. AGU, *84*(46), Fall Meet. Suppl., Abstract S52F-0174. *Int. J. Earth. Sci.*, *1-18*, doi:10.1007/s00531-013-0955-8.

Arroyo, I. G., G. E. Alvarado, and E. R. Flueh (2003), Local seismicity at the Cocos Ridge—Osa Peninsula Subduction Zone, Costa Rica, Abstract S52F-0174.

Arroyo, I. G., S. Husen, E. R. Flueh, J. Gossler, E. Kissling, and G. E. Alvarado (2009), Three-dimensional P-wave velocity structure on the shallow part of the Central Costa Rican Pacific margin from local earthquake tomography using off- and onshore networks, *Geophys. J. Int.*, *179*(2), 827–849, doi:10.1111/j.1365-246X.2009.04342.x.

Barckhausen, U., C. R. Ranero, R. von Huene, S. C. Cande, and H. A. Roeser (2001), Revised tectonic boundaries in the Cocos Plate off Costa Rica: Implications for the segmentation of the convergent margin and for plate tectonic models, *J. Geophys. Res.*, *106*(B9), 19,207–19,220, doi:10.1029/2001JB000238.

Bilek, S. L., and C. Lithgow-Bertelloni (2005), Stress changes in the Costa Rica subduction zone due to the 1999 Mw = 6.9 Quepos earthquake, *Earth Planet. Sci. Lett.*, *230*(1-2), 97-112, doi:10.1016/j.epsl.2004.11.020.

Bilek, S. L., S. Y. Schwartz, and H. R. DeShon (2003), Control of seafloor roughness on earthquake rupture behavior, *Geology*, *31*(5), 455–458, doi:10.1130/0091–7613(2003)031<0455:COSROE>2.0.CO;2.

DeMets, C., R. G. Gordon, D. F. Argus, and S. Stein (1994), Effect of recent revisions to the geomagnetic reversal time scale on estimates of current plate motions, *Geophys. Res. Lett.*, *21*(20), 2191–2194, doi:10.1029/94GL02118.

DeShon, H. R., S. Y. Schwartz, S. L. Bilek, L. M. Dorman, V. Gonzalez, J. M. Protti, E. R. Flueh, and T. H. Dixon (2003), Seismogenic zone structure of the southern Middle America Trench, Costa Rica, *J. Geophys. Res.*, *108*(B10), 2491, doi:10.1029/2002JB002294.

DeShon, H. R., S. Y. Schwartz, A. V. Newman, V. González, M. Protti, L. M. Dorman, T. H. Dixon, D. E. Sampson, and E. R. Flueh (2006), Seismogenic zone structure beneath the Nicoya Peninsula, Costa Rica, from three-dimensional local earthquake P- and S-wave tomography, *Geophys. J. Int.*, *164*(1), 109–124, doi:10.1111/j.1365-246X.2005.02809.x.

Dinc, A. N., I. Koulakov, M. Thorwart, W. Rabbel, E. R. Flueh, I. Arroyo, W. Taylor, and G. Alvarado (2010), Local earthquake tomography of central Costa Rica: Transition from seamount to ridge subduction, *Geophys. J. Int.*, *183*(1), 286–302, doi:10.1111/j.1365-246X.2010.04717.x.

Dziewonski, A. M., T. A. Chou, and J. H. Woodhouse (1981), Determination of earthquake source parameters from waveform data for studies of global and regional seismicity, *J. Geophys. Res.*, *86*(B4), 2825–2852, doi:10.1029/JB086iB04p02825.

Dzierma, Y., W. Rabbel, M. M. Thorwart, E. R. Flueh, M. M. Mora, and G. E. Alvarado (2011), The steeply subducting edge of the Cocos Ridge: Evidence from receiver functions beneath the northern Talamanca Range, south-central Costa Rica, *Geochem., Geophys., Geosyst.*, 12, Q04S30, doi:10.1029/2010GC003477.

Expedition 334 Scientists (2011), Costa Rica seismogenesis project (CRISP): Sampling and quantifying input to the seismogenic zone and fluid output, *Prelim. Rep. Integrated Ocean Drill. Program, 334*, doi:10.2204/iodp.pr.319.2009.

Expedition 344 Scientists (2013), Costa Rica Seismogenesis Project, Program A Stage 2 (CRISP-A2), *Prelim. Rep. Integr. Ocean Drill. Program, 344*, doi:10.2204/iodp.pr.334.2011.

Fernández Arce, M., and D. I. Doser (2009), Relocation and waveform modeling of the 1924 Orotina, Costa Rica, earthquake (MS 7.0), *Tectonophysics*, *479*(3-4), 197–202, doi:10.1016/j.tecto.2009.08.010.
Fisher, D. M., T. W. Gardner, P. B. Sak, J. D. Sanchez, K. Murphy, and P. Vannucchi (2004), Active thrusting in the inner forearc of an erosive convergent margin, Pacific coast, Costa Rica, *Tectonics*, *23*, TC2007, doi:10.1029/2002TC001464.
Fujiwara, T., S. Kodaira, T. No, Y. Kaiho, N. Takahashi, and Y. Kaneda (2011), The 2011 Tohoku-Oki Earthquake: Displacement reaching the trench axis, *Science*, *334*(6060), 1240–1240, doi:10.1126/science.1211554.
Gomberg, J. S., K. M. Shedlock, and S. W. Roecker (1990), The effect of S-wave arrival times on the accuracy of hypocenter estimation, *Bull. Seismol. Soc. Am.*, *80*(6A), 1605–1628.
Harris, R. N., G. Spinelli, C. R. Ranero, I. Grevemeyer, H. Villinger, and U. Barckhausen (2010), Thermal regime of the Costa Rican convergent margin: 2. Thermal models of the shallow Middle America subduction zone offshore Costa Rica, *Geochem. Geophys. Geosyst. 11*, Q12S29, doi:10.1029/2010GC003273.
Haslinger, F., E. Kissling, J. Ansorge, D. Hatzfeld, E. Papadimitriou, V. Karakostas, K. Makropoulos, H. G. Kahle, and Y. Peter (1999), 3D crustal structure from local earthquake tomography around the Gulf of Arta (Ionian region, NW Greece), *Tectonophysics*, *304*(3), 201–218, doi:10.1016/S0040-1951(98)00298-4.
Husen, S., and R. B. Smith (2004), Probabilistic earthquake relocation in three-dimensional velocity models for the Yellowstone National Park Region, Wyoming, *Bull. Seismol. Soc. Am.*, *94*(3), 880–896, doi:10.1785/0120030170.
Husen, S., E. Kissling, and R. Quintero (2002), Tomographic evidence for a subducted seamount beneath the Gulf of Nicoya, Costa Rica: The cause of the 1990 Mw = 7.0 Gulf of Nicoya earthquake, *Geophys. Res. Lett.*, *29*(8), 1238, doi:10.1029/2001GL014045.
Husen, S., R. Quintero, E. Kissling, and B. Hacker (2003), Subduction-zone structure and magmatic processes beneath Costa Rica constrained by local earthquake tomography and petrological modelling, *Geophys. J. Int.*, *155*(1), 11–32, doi:10.1046/j.1365-246X.2003.01984.x.
Hyndman, R. D., K. Wang, and M. Yamano (1995), Thermal constraints on the seismogenic portion of the southwestern Japan subduction thrust, *J. Geophys. Res.*, *100*(B8), 15,373–15,392, doi:10.1029/95JB00153.
Ide, S., A. Baltay, and G. C. Beroza (2011), Shallow dynamic overshoot and energetic deep rupture in the 2011 Mw 9.0 Tohoku-Oki Earthquake, *Science*, *332*(6036), 1426–1429, doi:10.1126/science.1207020.
Kennett, B. L. N., E. R. Engdahl, and R. Buland (1995), Constraints on seismic velocities in the Earth from traveltimes, *Geophys. J. Int.*, *122*(1), 108–124, doi:10.1111/j.1365-246X.1995.tb03540.x.
Kikuchi, M., and M. Ishida (1993), Source retrieval for deep local earthquakes with broadband records, *Bull. Seismol. Soc. Am.*, *83*(6), 1855–1870.
Kikuchi, M., and H. Kanamori (1991), Inversion of complex body waves-III, *Bull. Seismol. Soc. Am.*, *81*(6), 2335–2350.
Kissling, E., W. L. Ellsworth, D. Eberhart-Phillips, and U. Kradolfer (1994), Initial reference models in local earthquake tomography, *J. Geophys. Res.*, *99*(B10), 19,635–19,646, doi:10.1029/93JB03138.
Kluesner, J. W., E. A. Silver, N. L. Bangs, K. D. McIntosh, J. Gibson, D. Orange, C. R. Ranero, and R. von Huene (2013), High density of structurally controlled, shallow to deep water fluid seep indicators imaged offshore Costa Rica, *Geochem. Geophys. Geosyst.*, *14*, 519–539, doi:10.1002/ggge.20058.
Kolarsky, R. A., P. Mann, and W. Montero (1995), Island arc response to shallow subduction of the Cocos Ridge, in *Geologic and Tectonic Development of the Caribbean Plate Boundary in Southern Central America*, edited by P. Mann, pp. 235–262, *Geol. Soc. of Am.*, doi:10.1130/SPE295-p235.
LaFemina, P., T. H. Dixon, R. Govers, E. Norabuena, H. Turner, A. Saballos, G. Mattioli, M. Protti, and W. Strauch (2009), Fore-arc motion and Cocos Ridge collision in Central America, *Geochem. Geophys. Geosyst. 10*, Q05S14, doi:10.1029/2008GC002181.
Lienert, B. R., and J. Havskov (1995), A computer program for locating earthquakes both locally and globally, *Seismol. Res. Lett.*, *66*(5), 26–36, doi:10.1785/gssrl.66.5.26.
Linkimer, L., I. Arroyo, M. M. Mora, A. Vargas, G. J. Soto, R. Barquero, W. Rojas, W. Taylor, and M. Taylor (2013), El terremoto de Sámara (Costa Rica) del 5 de setiembre del 2012 (Mw 7,6), *Rev. Geol. Am. Cent.*, *49*, 73–82.
Lomax, A., J. Virieux, P. Volant, and C. Berge-Thierry (2000), Probabilistic earthquake location in 3D and layered models, in *Advances in Seismic Event Location*, edited by C. H. Thurber and N. Rabinowitz, pp. 101–134, Kluwer Acad., Dordrecht, Netherlands.
Loveless, J. P., and B. J. Meade (2011), Spatial correlation of interseismic coupling and coseismic rupture extent of the 2011 MW = 9.0 Tohoku-oki earthquake, *Geophys. Res. Lett.*, *38*, L17306, doi:10.1029/2011GL048561.
Lücke, O. (2012), 3D density modeling of the Central American Isthmus from satellite derived gravity data, PhD thesis, Christian-Albrechts-Universität zu Kiel, Kiel, Germany.
MacMillan, I., P. B. Gans, and G. Alvarado (2004), Middle Miocene to present plate tectonic history of the southern Central American Volcanic Arc, *Tectonophysics*, *392*(1-4), 325–348, doi:10.1016/j.tecto.2004.04.014.
Morell, K. D., E. Kirby, D. M. Fisher, and M. van Soest (2012), Geomorphic and exhumational response of the Central American Volcanic Arc to Cocos Ridge subduction, *J. Geophys. Res.*, *117*(B4), B04409, doi:10.1029/2011JB008969.
Moore, J. C., and D. Saffer (2001), Updip limit of the seismogenic zone beneath the accretionary prism of southwest Japan: An effect of diagenetic to low-grade metamorphic processes and increasing effective stress, *Geology*, *29*(2), 183–186, doi:10.1130/0091-7613(2001)029<0183:ulotsz>2.0.co;2.
Moore, J. C., C. Rowe, and F. Meneghini (2007), How Accretionary Prisms Elucidate Seismogenesis in Subduction Zones, in *The Seismogenic Zone of Subduction Thrust Faults*, edited by T. H. Dixon and J. C. Moore, pp. 288–315, Columbia University Press, N.Y.
Moser, T. J., T. van Eck, and G. Nolet (1992), Hypocenter determination in strongly heterogeneous earth models using the shortest path method, *J. Geophys. Res.*, *97*(B5), 6563–6572, doi:10.1029/91JB03176.
Oleskevich, D. A., R. D. Hyndman, and K. Wang (1999), The updip and downdip limits to great subduction earthquakes: Thermal and structural models of Cascadia, south Alaska, SW Japan, and Chile, *J. Geophys. Res.*, *104*(B7), 14,965–14,991, doi:10.1029/1999JB900060.
Ottemöller, L., P. Voss, and J. Havskov (2012), *SEISAN Earthquake Analysis Software for Windows, Solaris, Linux and MacOSX*, Version 9.1, Univ. of Bergen, Bergen, Norway.
Quintero, R., and E. Kissling (2001), An improved P-wave velocity reference model for Costa Rica, *Geofís. Int.*, *40*, 3–19.
Ranero, C., P. Vannucchi, and R. von Huene (2007), Drilling the seismogenic zone of an Erosional convergent margin: IODP Costa Rica Seismogenesis Project CRISP, in *Abstracts and Report From the IODP/ICDP Workshop on Fault Zone Drilling*, edited, Special Edition N.1. pp. 51–54, Integrated Ocean Drill. Program Manage. Int., Miyzaki, Japan.
Ranero, C. R., and R. von Huene (2000), Subduction erosion along the Middle America convergent margin, *Nature*, *404*(6779), 748–752, doi:10.1038/35008046.

Ranero, C. R., I. Grevemeyer, H. Sahling, U. Barckhausen, C. Hensen, K. Wallmann, W. Weinrebe, P. Vannucchi, R. von Huene, and K. McIntosh (2008), Hydrogeological system of erosional convergent margins and its influence on tectonics and interplate seismogenesis, *Geochem. Geophys. Geosyst. 9*, Q03S04, doi:10.1029/2007GC001679.

Sak, P. B., D. M. Fisher, T. W. Gardner, J. S. Marshall, and P. C. LaFemina (2009), Rough crust subduction, forearc kinematics, and Quaternary uplift rates, Costa Rican segment of the Middle American Trench, *Geol. Soc. Am. Bull.*, *121*(7-8), 992–1012, doi:10.1130/B26237.1.

Sallarès, V., P. Charvis, E. R. Flueh, and J. Bialas (2003), Seismic structure of Cocos and Malpelo Volcanic Ridges and implications for hot spot-ridge interaction, *J. Geophys. Res.*, *108*(B12), 2564, doi:10.1029/2003JB002431.

Sitchler, J. C., D. M. Fisher, T. W. Gardner, and M. Protti (2007), Constraints on inner forearc deformation from balanced cross sections, Fila Costeña thrust belt, Costa Rica, *Tectonics*, *26*, TC6012, doi:10.1029/2006TC001949.

Stavenhagen, A. U., E. R. Flueh, C. Ranero, K. D. McIntosh, T. Shipley, G. Leandro, A. Schultze, and J. J. Dañobeitia (1998), Seismic wide-angle investigations in Costa Rica—A crustal velocity model from the Pacific to the Caribbean, *Zent. Geol. Paläontol.*, *3-6*(Teil 1), 393–408.

Tarantola, A., and B. Valette (1982), Inverse problems = Quest for information, *J. Geophys.*, *50*, 159–170.

Vannucchi, P., K. Ujiie, N. Stroncik, A. Malinverno, and E. Scientists (2012), Costa Rica Seismogenesis Project, Program A Stage 1 (CRISP-A1), in Proceedings of the Integrated Ocean Drill. Program Manage, *334*, doi: 10.2204/iodp.proc.334.2012.

Vannucchi, P., P. B. Sak, J. P. Morgan, K. I. Ohkushi, K. Ujiie, and I. E. S. S. The (2013), Rapid pulses of uplift, subsidence, and subduction erosion offshore Central America: Implications for building the rock record of convergent margins, *Geology*, *41*(9), 995–998, doi:10.1130/G34355.1.

von Huene, R., C. R. Ranero, W. Weinrebe, and K. Hinz (2000), Quaternary convergent margin tectonics of Costa Rica, segmentation of the Cocos Plate, and Central American volcanism, Tectonics, *19*, 314–334, doi:10.1029/1999TC001143.

von Huene, R., C. R. Ranero, and P. Vannucchi (2004), Generic model of subduction erosion, *Geology*, *32*(10), 913–916, doi:10.1130/G20563.1.

Walther, C. H. E. (2003), The crustal structure of the Cocos ridge off Costa Rica, *J. Geophys. Res.*, *108*(B3), 2136, doi:10.1029/2001JB000888.

Wang, K., and S. L. Bilek (2014), Invited review paper: Fault creep caused by subduction of rough seafloor relief, *Tectonophysics*, *610*, 1–24, doi:10.1016/j.tecto.2013.11.024.

Wessel, P., and W. H. F. Smith (1998), New, improved version of generic mapping tools released, *Eos Trans AGU*, *79*(47), 579–579, doi:10.1029/98EO00426.

Ye, S., J. Bialas, E. R. Flueh, A. Stavenhagen, R. von Huene, G. Leandro, and K. Hinz (1996), Crustal structure of the Middle American Trench off Costa Rica from wide-angle seismic data, *Tectonics*, *15*(5), 1006–1021, doi:10.1029/96TC00827.

Yue, H., and T. Lay (2013), Source rupture models for the Mw 9.0 2011 Tohoku Earthquake from joint inversions of high-rate geodetic and seismic data, *Bull. Seismol. Soc. Am.*, *103*(2B), 1242–1255, doi:10.1785/0120120119.